Electronic Supplementary Information

Modelling the Activity Trend of Hydrogen Oxidation Reaction under Constant Potential Conditions

Wenhui Ling, Jian Liu, and Bo Yang*

School of Physical Science and Technology, ShanghaiTech University, 393 Middle Huaxia Road, Shanghai 201210, China

*Email: yangbo1@shanghaitech.edu.cn

1. Density functional theory calculations

For all density functional theory (DFT) calculations, the Vienna Ab-initio Simulation Package (VASP)[1, 2] was utilized, employing the Projector Augmented-Wave (PAW) method[3, 4] to model electron-ion interactions. To approximate exchange and correlation energies, the Perdew-Burke Ernzerhof (PBE) functional[5] was utilized. A cutoff energy of 400 eV was used, and a convergence criterion for forces of 0.05 eV/Å was applied. A minimum vacuum height of 13 Å was imposed to prevent interactions between periodic structures. The energy associated with the most stable configuration was used in the calculation of free energy for various adsorbates, and the nudged elastic band (NEB)[6] method was employed to locate transition states.

Simulations conducted under constant potential conditions were performed using the grand-canonical density functional theory (GC-DFT)[7] method within the JDFTx software package.[8] The PBE functional was also used here, and an energy cutoff of 14.7 Hartree (400 eV) was employed. Brillouin zone sampling utilized the Monkhorst-Pack scheme[1]. To account for solvation effects, the implicit solvent model CANDLE[9] was employed, with the implicit solvent environment[10-13] providing compensating charges to maintain overall charge neutrality within the unit cell. The parameters were configured for a solvent environment containing 1 M fluoride anions and 1 M sodium cations in an aqueous solution. Additionally, we opted to include two explicit water molecules in the model. On one hand, the implicit solvent model represents the solvent as a continuous medium, simplifying the system complexity and improving computational efficiency. On the other hand, incorporating a small number of explicit water molecules provides a more detailed and accurate description, especially around active sites or key reaction sites, thereby balancing efficiency and accuracy.[14-16]

2. Adsorption energy calculations

The free energy of hydrogen adsorption ($H_2 + 2* \rightarrow 2H^*$) was calculated using the following equation:

$$\Delta G_{H^*} = \frac{1}{2}E_{slab+2H^*} - E_{H_2} - E_{slab} + TS_{H_2} \quad \text{(S1)}$$

where $E_{slab+2H*}$ and E_{slab} are the energies of the slab with adsorbed $2H^*$ and the clean slab, respectively. E_{H_2} denotes the energy of gaseous H_2, while S_{H_2} signifies the entropy of H_2 at 298.15 K, which is 1.36 meV/K.

The activity descriptor of the catalyst should be formulated in a manner that is both straightforward and computationally efficient. We begin by considering the OH adsorption process: $H_2O + * \rightarrow OH^* + \frac{1}{2}H_2$

Based on this equation, the OH adsorption energy can be calculated using the following expression:

$$\Delta G_{OH^*} = E_{slab+OH^*} + \frac{1}{2}G_{H_2} - G_{H_2O} - E_{slab} \quad \text{(S2)}$$

where $E_{slab+OH^*}$ is the total energy of the slab with absorbed OH*, while G_{H_2} and G_{H_2O} are the Gibbs free energy of H_2(g) and H_2O(l), respectively, which can be calculated using the following equations:

$$G_{H_2} = E_{H_2} - TS_{H_2}$$

$$G_{H_2O} = E_{H_2O} - TS_{H_2O}$$

In the context of this straightforward model, the adsorption process of OH does not involve electron transfer, resulting in exceptionally high computational efficiency for determining the adsorption energy.

By constructing a thermodynamic cycle, we can derive the following relationships:

$$\Delta G_{OH^-} = \Delta G_{OH^*} + G_{H_2O} - \frac{1}{2}G_{H_2} - G_{OH^-} + G_{e^-} \quad \text{(S3)}$$

therefore, we can have

$\Delta G_{OH^-} - \Delta G_{OH^*} = G_{H_2O} - \frac{1}{2}G_{H_2} - G_{OH^-} + G_{e^-} = 0.83\ eV + eU$, according to the standard Gibbs energy of formation of H_2O, H_2 and OH^- at 298.15 K. When the electrode potentials are at 0 V and 0.2 V vs. RHE, we can derive: $\Delta G_{OH^-} - \Delta G_{OH^*} = 0.83\ eV$ and $\Delta G_{OH^-} - \Delta G_{OH^*} = 1.03\ eV$, respectively.

3. Microkinetic simulation

Previous researchers have extensively demonstrated that microkinetic model can help determine the rates of specific steps of catalytic reactions, including reactant adsorption, activation, and the formation of reaction intermediates.[16-19] We employed a similar approach to perform Microkinetic simulation. The rate-determining step (RDS) would be one of the steps within the Tafel step, Indirect Volmer step or Direct Volmer step.

$$\frac{1}{2}H_2 + * \rightarrow H^* \quad (1)$$

$$H^* + OH^* \rightarrow H_2O + 2* \quad (2)$$

$$H^* + OH^- \rightarrow H_2O + e^- + * \quad (3)$$

An additional OH^- adsorption process is involved in Indirect Volmer step:

$$OH^- + * \rightarrow OH^* + e^- \quad (4)$$

When step (1) is rate-determining in the reaction, other steps are considered quasi-equilibrated, then we can have

$r = r_1 = k_1\theta^*$, and $k_1 = Aexp(-\frac{\Delta G_{TS}^H}{RT})$

$$\theta^* = \frac{K_4K_2}{1 + K_4K_2 + K_4^2K_2}, \quad K_4 = \exp\left(-\frac{\Delta G_{OH^-}}{RT}\right), \quad K_2 = \exp\left(\frac{\left(\Delta G_{H^*} + \Delta G_{OH^-}\right)}{RT}\right)$$

It should be noted that step (2) and step (3) are competing in the system, therefore one can consider the rate-determining step being either step (2) or step (3).

When step (2) is rate-determining, we can have

$r = r_2 = k_2\theta_H\theta_{OH}$, and $k_2 = Aexp\left(\frac{\Delta G_{H^*} + \Delta G_{OH^-}}{RT}\right)$

$\theta_H = \sqrt{p/p^0}K_1\theta^*$, $\theta_{OH} = cK_4\theta^*$, $K_1 = exp\left(-\frac{\Delta G_{H^*}}{RT}\right)$, $K_4 = \exp\left(-\frac{\Delta G_{OH^-}}{RT}\right)$,

$$\theta^* = \frac{1}{1 + exp\left(-\frac{\Delta G_{H^*}}{RT}\right) + \exp\left(-\frac{\Delta G_{OH^-}}{RT}\right)}$$

Similarly, when step (3) is rate-determining, step (1) is considered quasi-equilibrated, the following relations can be obtained:

$r = r_3 = k_3\theta_H$, and $k_3 = Aexp\left(-\frac{\Delta G_{TS}}{RT}\right)$, $\theta_H = \frac{K_1}{1 + K_1}$, $K_1 = Aexp\left(-\frac{\Delta G_{H*}}{RT}\right)$

In the above expressions, k_i and K_i indicate the forward rate constant and equilibrium constant of step i, respectively. p (1 bar in the current work) and θ indicates the pressure and intermediates coverage, respectively. p^0 represents the standard pressure, i.e., 1 bar. c is the molar concentration of OH^-, which is 0.1 mol/L in the current work, corresponding to pH = 13. ΔG_{TS}^{H} and ΔG_{TS} represent the activation energies of the Tafel and Volmer steps, respectively. ΔG_{H^*} and ΔG_{OH^-} represent the adsorption energies of H and OH^-, respectively. The corresponding rate constants (k) and coverage(θ) can be calculated as functions of H adsorption energy (G_{H^*})and OH adsorption energy (ΔG_{OH^*}), with the specific functional relationships provided in Figure 3 of the main text. A is the pre-exponential factor which is $\frac{k_B T}{h}$, k_B and h represent Boltzmann and Planck constant. The overall reaction rate is given by $\min(r_1, \max(r_2, r_3))$. The basic idea is that the overall rate should be equal to the rate of the rate determining step, which shows the lowest reaction rate in the whole reaction pathway and the method has been used in the microkinetic analyses of electrocatalytic reactions.[16, 17, 20]

Table S1. Adsorption free energies of H and OH on different catalyst surfaces.

	ΔG_{H*}/eV	ΔG_{OH*}/eV
Cu(111)	-0.03	0.90
Ag(111)	0.40	0.95
Au(111)	0.32	1.55
Pt(111)	-0.24	1.11
Pd(111)	-0.51	0.70
Ir(111)	-0.17	0.79
Rh(111)	-0.32	0.34
Ru(0001)	-0.41	-0.14
PtRu	-0.30	0.41
PdNi	-0.28	0.13
SnRu	-0.39	0.05
RuNi	-0.45	-0.21
PtRu(alloy)	-0.26	0.05
GaRu	-0.43	-0.17
PdIr2	-0.33	0.45
IrRu2	-0.34	0.13
Ir_1Ru_1	-0.41	-0.03
PtCu	0.02	1.34
PtAu	-0.52	0.44
NiCu	-0.37	0.03
PtRu	-0.30	0.41
WNi_4	-0.30	-1.31
$MoNi_4$	-0.29	-0.88
$1OH_W$	-0.38	-1.25
$1OH_{Mo}$	-0.37	-0.41
$2OH_W$	-0.49	-0.42
$2OH_{Mo}$	-0.48	0.24

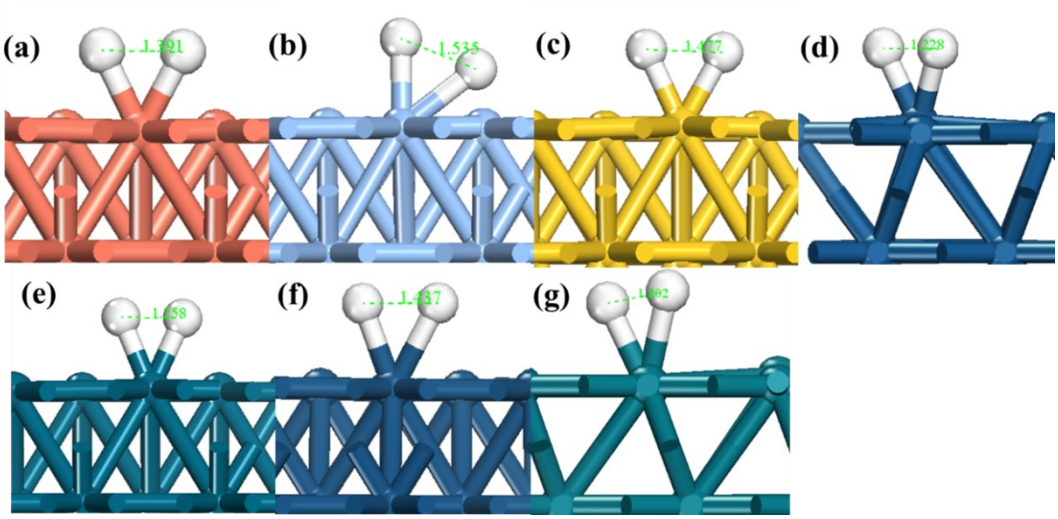

Figure S1. Structure of H_2 dissociation step transition state on (a) Cu(111), (b) Ag(111), (c)Au (111), (d) Pt(111), (e) Pd(111), (f) Ir (111) and (g) Rh(111) surfaces. White balls are hydrogen atoms.

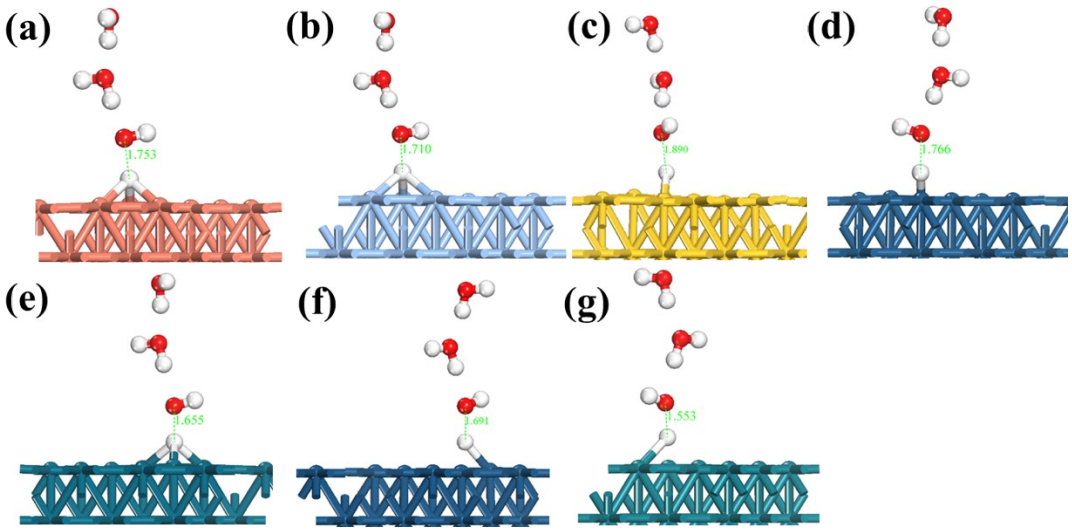

Figure S2. Structure of the Direct Volmer step transition state on (a) Cu(111), (b) Ag(111), (c)Au (111), (d) Pt(111), (e) Pd(111), (e) Ir (111) and (g) Rh(111) surfaces. Red and white balls are oxygen and hydrogen atoms, respectively.

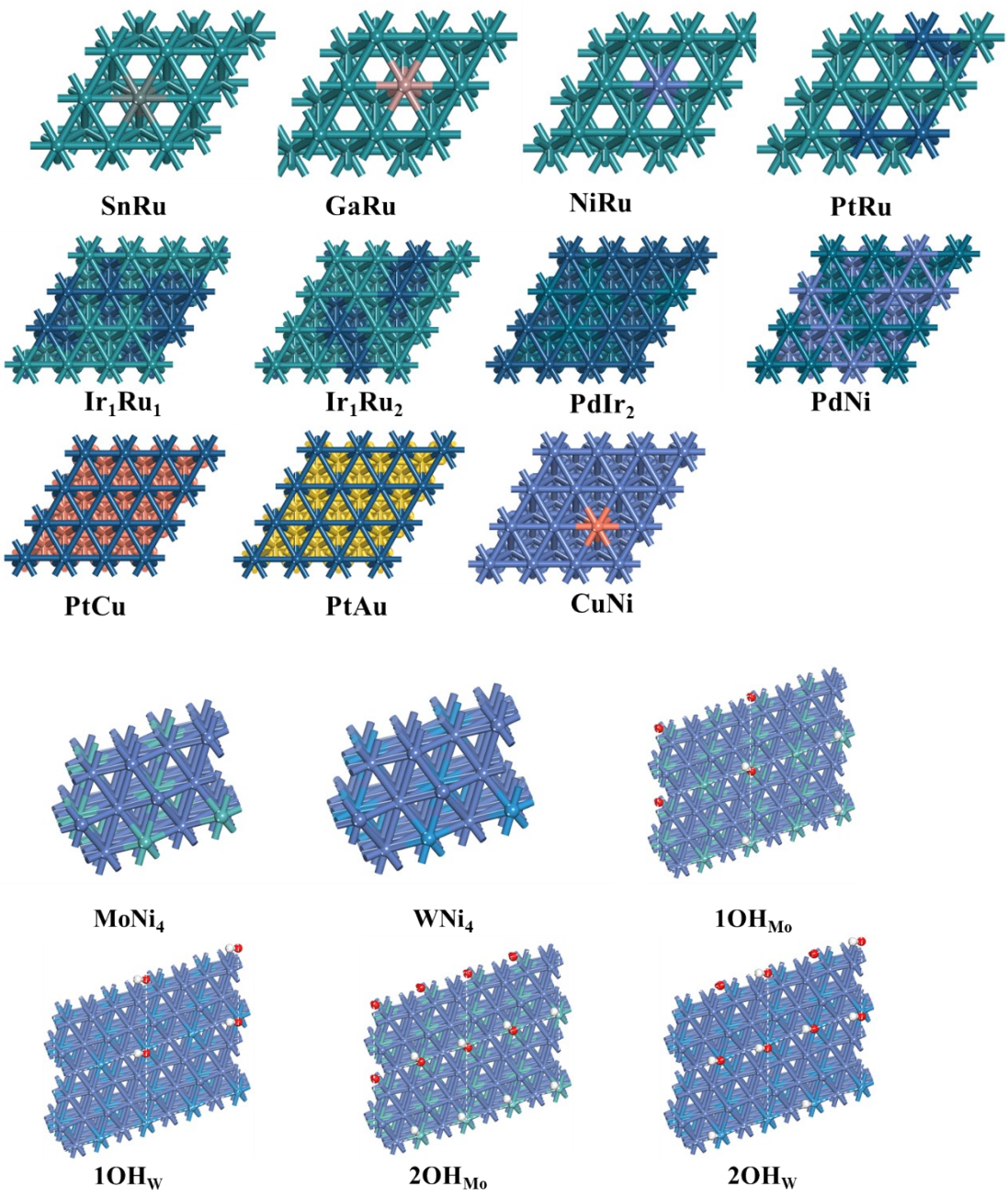

Figure S3. Structure of alloy catalysts.

5. Input file

Our input files include three types: the first type is the DFT calculation for structural optimization using VASP, the second type uses NEB for transition state search, and the third type conducts simulations under constant potential conditions using JDFTx. Below is the example input file we provided:

#DFT input file

general:

System = Cu

ISTART=0

ISPIN=1

ENCUT = 400 eV

PREC=high

ISIF=2

IBRION=2

POTIM=0.2

ALGO=Fast

EDIFFG=-0.05

ISMEAR = 1; SIGMA = 0.10

NSW = 2000

LREAL=A

LWAVE =.False.

GGA=PE

NELM=200

NSIM=4

LCHARG = F

ISYM = 0

LSOL = .TRUE.

EB_K = 80

#NEB input file

general:

System = Cu

ISTART=0

ISPIN=1

ENCUT = 400 eV

PREC=high

ISIF=2

IBRION=3 #2sructure-opt 3-neb

POTIM=0

#IALGO = 48

ALGO=Fast

EDIFF=1E-7

EDIFFG=-0.03

ISMEAR = 1; SIGMA = 0.10

NSW = 2000

LREAL=A

LWAVE =.False.

GGA=PE

NELM=200

NSIM=4

LCHARG = F

ISYM = 0

LSOL = .TRUE.

EB_K = 80

ICHAIN=0

IPOT=1

IMAGES=7

SPRING=-5

LCLIMB=.False.

#JDFTx inputfile

```
#--- Pseudopotentials ---
ion-species GBRV/$ID_pbe.uspp    #GBRV family
elec-cutoff 14.7                 #Ecuts for psi and rho
elec-ex-corr gga-PBE
include in.lattice
include in.ionpos
coulomb-truncation-ion-margin 4
ionic-minimize \
    nIterations 2000 \
    energyDiffThreshold 0 \
    knormThreshold 1e-3    #Threshold on RMS cartesian force
#--- Electronic ---
kpoint-folding 3 3 1
elec-smearing MP1 0.00184
target-mu -0.1349 #-0.1422 for 0.2V
#--- Fluid ---
fluid LinearPCM
pcm-variant CANDLE
fluid-solvent H2O
fluid-cation Na+ 0.1
fluid-anion F- 0.1
dump-name opt.$VAR
dump End IonicPositions
dump End ElecDensity
```

References

1. G. Kresse and J. Furthmüller, *Phys. Rev. B*, 1996, **54**, 11169-11186.
2. G. Kresse and J. Furthmüller, *Comput. Mater. Sci.*, 1996, **6**, 15-50.
3. P. E. Blöchl, *Phys. Rev. B*, 1994, **50**, 17953-17979.
4. G. Kresse and D. Joubert, *Phys. Rev. B*, 1999, **59**, 1758-1775.
5. J. P. Perdew, K. Burke and M. Ernzerhof, *Phys. Rev. Lett.*, 1996, **77**, 3865-3868.
6. G. Henkelman, B. P. Uberuaga and H. Jónsson, *J. Chem. Phys.*, 2000, **113**, 9901-9904.
7. R. Sundararaman, W. A. Goddard, III and T. A. Arias, *J. Chem. Phys.*, 2017, **146**.
8. R. Sundararaman, K. Letchworth-Weaver, K. A. Schwarz, D. Gunceler, Y. Ozhabes and T. A. Arias, *SoftwareX*, 2017, **6**, 278-284.
9. R. Sundararaman and W. A. Goddard, III, *J. Chem. Phys.*, 2015, **142**, 064107.
10. Y. Basdogan, A. M. Maldonado and J. A. Keith, 2020, **10**, e1446.
11. G. Fisicaro, L. Genovese, O. Andreussi, N. Marzari and S. Goedecker, *J Chem Phys*, 2016, **144**, 014103.
12. Y.-H. Fang and Z.-P. Liu, *J. Phys. Chem. C*, 2009, **113**, 9765-9772.
13. A. Y. Lozovoi, A. Alavi, J. Kohanoff and R. M. Lynden-Bell, *J. Chem. Phys.*, 2001, **115**, 1661-1669.
14. M. Li, L. Li, X. Huang, X. Qi, M. Deng, S. Jiang and Z. Wei, *J. Phys. Chem. Lett.*, 2022, **13**, 10550-10557.
15. L. Han, P. Ou, W. Liu, X. Wang, H.-T. Wang, R. Zhang, C.-W. Pao, X. Liu, W.-F. Pong, J. Song, Z. Zhuang, M. V. Mirkin, J. Luo and H. L. Xin, *Sci. Adv.*, **8**, eabm3779.
16. I. T. McCrum and M. T. M. Koper, *Nat. Energy*, 2020, **5**, 891-899.
17. J. Li, H. Liu, J. Liu and B. Yang, *Mater. Today Chem.*, 2023, **29**, 101461.
18. H. Liu and B. Yang, *Chem. Commun.*, 2022, **58**, 709-712.
19. C. Tsai, K. Lee, J. S. Yoo, X. Liu, H. Aljama, L. D. Chen, C. F. Dickens, T. S. Geisler, C. J. Guido, T. M. Joseph, C. S. Kirk, A. A. Latimer, B. Loong, R. J. McCarty, J. H. Montoya, L. Power, A. R. Singh, J. J. Willis, M. M. Winterkorn,

M. Yuan, Z.-J. Zhao, J. Wilcox and J. K. Nørskov, *Catal. Lett.*, 2016, **146**, 718-724.

20. H. A. Hansen, J. B. Varley, A. A. Peterson and J. K. Nørskov, *J. Phys. Chem. Lett.*, 2013, **4**, 388-392.